

AD-A172 973

MECHANISMS OF EXHAUST POLLUTANTS AND PLUME FORMATION IN

1/1

CONTINUOUS COMBUS. (U) CALIFORNIA UNIV IRVINE

COMBUSTION LAB G. J. SAMUELSEN 30 NOV 84 UCI-ART-84-18

UNCLASSIFIED

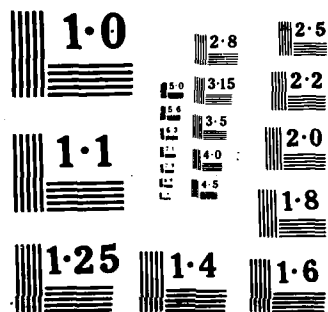
AFOSR-IR-86-0883 AFOSR-84-0202

F/G 21/2

NL

1002

END
DATE
FILMED
11-86



2

AFOSR-TR- 86-0883

AD-A172 973

AIR FORCE OFFICE OF SCIENTIFIC RESEARCH (AFOSR)
NOTICE OF TRANSMITTAL TO DTIC

This technical report has been reviewed and is
Approved for public release IAW AFR 190-12.
Distribution is unlimited.

MATTHEW J. KERTER

Chief, Technical Information Division

Approved for public release;
distribution unlimited.

MECHANISMS OF EXHAUST POLLUTANTS AND PLUME FORMATION
IN CONTINUOUS COMBUSTION

G.S. Samuelsen
Principal Investigator

AFOSR Grant 83-0202
Air Force Office of Scientific Research (AFOSR)
Bolling AFB, Washington, D.C. 20332

UCI-ARTR-84-18

November 1984

DTIC
ELECTE
OCT 9 1986
B

COMBUSTION INVESTIGATOR

Mechanical Engineering
University of California
Irvine 92717



DTIC FILE COPY

86 10 8 095

Unclassified

SECURITY CLASSIFICATION OF THIS PAGE

AD A172 913

REPORT DOCUMENTATION PAGE				
1a. REPORT SECURITY CLASSIFICATION Unclassified			1d. RESTRICTIVE MARKINGS	
2a. SECURITY CLASSIFICATION AUTHORITY			3. DISTRIBUTION/AVAILABILITY OF REPORT Approved for public release; distribution unlimited	
2b. DECLASSIFICATION/DOWNGRADING SCHEDULE				
4. PERFORMING ORGANIZATION REPORT NUMBER(S) ARTR-84-18			5. MONITORING ORGANIZATION REPORT NUMBER(S) AFOSR-TR. 86-0883	
6a. NAME OF PERFORMING ORGANIZATION University of California UCI Combustion Laboratory		6b. OFFICE SYMBOL (If applicable)	7a. NAME OF MONITORING ORGANIZATION Air Force Office of Scientific Research	
6c. ADDRESS (City, State and ZIP Code) Mechanical Engineering University of California Irvine, California 92717		7b. ADDRESS (City, State and ZIP Code) AFOSR/NA Bolling AFB, Washington, D.C. 20332-6448		
8a. NAME OF FUNDING/SPONSORING ORGANIZATION Air Force Office of Scientific Research		8b. OFFICE SYMBOL (If applicable) NA	9. PROCUREMENT INSTRUMENT IDENTIFICATION NUMBER AFOSR 83-0202	
8c. ADDRESS (City, State and ZIP Code) Bolling AFB Washington, D.C. 20332 - 6448		10. SOURCE OF FUNDING NOS.		
		PROGRAM ELEMENT NO. 61102F	PROJECT NO. 2308	TASK NO. A2
				WORK UNIT NO.
11. TITLE (Include Security Classification) Mechanisms of Exhaust Pollutants and Plume Formation in Continuous Combustion				
12. PERSONAL AUTHOR(S) G.S. Samuelson				
13a. TYPE OF REPORT Final		13b. TIME COVERED FROM 05-83 TO 07-84	14. DATE OF REPORT (Yr., Mo., Day) 1984, November, 30	15. PAGE COUNT 54
16. SUPPLEMENTARY NOTATION				
17. COSATI CODES			18. SUBJECT TERMS (Continue on reverse if necessary and identify by block number)	
FIELD	GROUP	SUB. GR.		
21	01		Combustion and Ignition Sampling Gas Turbine	
21	02		Pollutants Formation Complex Flows Engines	
			Modeling Air Breathing Engines Sprays	
19. ABSTRACT (Continue on reverse if necessary and identify by block number) The development of combustors that are both fuel efficient and fuel flexible requires spatially resolved measurements of velocity, temperature, gas concentration, and droplet size and velocity in complex flows. Such data are needed to provide the physical insight necessary to understand the basic processes of turbulent transport and spray mechanics, and to support the evolution of modeling. The goals of the AFOSR program at the UCI Combustion Laboratory was to develop laboratory model combustors and experimental methodology suitable for the acquisition of the desired information. In a prior AFOSR study, a model laboratory combustor was developed and employed to study turbulent transport in gaseous-fired, swirl-stabilized reacting flows. The present grant was directed to operating the model combustor on spray-atomized liquid fuels, to establishing a droplet sizing capability that would lead to in-situ measurements of drop size and drop velocity within the				
20. DISTRIBUTION/AVAILABILITY OF ABSTRACT UNCLASSIFIED/UNLIMITED <input type="checkbox"/> SAME AS RPT. <input type="checkbox"/> DTIC USERS <input type="checkbox"/>			21. ABSTRACT SECURITY CLASSIFICATION	
22a. NAME OF RESPONSIBLE INDIVIDUAL Julian M Tushkoff			22b. TELEPHONE NUMBER (Include Area Code) 202 767-4935	22c. OFFICE SYMBOL NA

DD FORM 1473, 83 APR

EDITION OF 1 JAN 73 IS OBSOLETE.

Unclassified

SECURITY CLASSIFICATION OF THIS PAGE

combustor, and to the study of turbulent transport in swirl-stabilized, liquid-fuel spray-atomized reacting flows. The objectives of the program were (1) to develop and verify a capability to conduct in-situ measurements of droplet size and velocity, (2) to operate the model laboratory combustor with a liquid, spray-atomized twin-fluid nozzle, and (3) to conduct supplementary studies in support of the Air Force laboratory interests in complex flows.

The first objective was met by establishing the applicability of a non-intrusive, visibility technique with intensity validation (IV) for obtaining droplet size and velocity information within a practical liquid spray. Such measurements are useful to hardware designers as well as to those who model two-phase flow fields. However, for measurements to be conducted, (1) a calibration device such as a single-size droplet generator is indispensable in establishing the capabilities of an interferometric sizing system, (2) an alternate sizing method is necessary to complement and validate the visibility measurement in a dense spray environment, and (3) shadow photographs are valuable as a means of visually checking the sizes of drops within the spray and also indicate where measurements are not possible due to the asphericity of the droplets. It was found that a rotating grating can be effectively used as a beam splitter for an interferometric sizing system. Further, given the restriction of having to process signals within fairly narrow frequency bands, the variable frequency shift capability associated with the rotating grating is most appealing. The SMD determined by a laser diffraction technique (Malvern) was within the extremes of the radial variation of SMD generated by the visibility/IV technique. In addition, the distribution of the liquid mass within the spray as measured by the visibility/IV technique was qualitatively similar to a Rosin Rammler curve fit of the Malvern data at both axial stations.

The second objective was met by a study of the relationship between nozzle performance and the performance of a swirl-stabilized model laboratory combustor. The results established that air-assist nozzles exhibit a trend of improved atomization performance with increasing nozzle air-to-fuel ratio (A/F) similar to that observed for air-blast atomizers, and the size distribution of air-assist nozzles narrows with increasing A/F and increasing fuel flow rate. The performance of the model laboratory swirl-stabilized combustor increased with A/F due to improved atomization (lower droplet sizes and narrower size distributions) and higher fuel momentum. An A/F ratio was reached, above which the combustor could not be stabilized and "flamed-out". An intrinsic asymmetry, introduced into the nozzle, was not reflected in laser diffraction measurements of SMD but rather in patternator measurements of mass flux. The nozzle asymmetry was also observed in the radial profiles of gaseous species emitted from the combustor. Quantification of the combustor velocity field as a function of nozzle operating condition will be required, along with droplet size and droplet velocity measurements, to relate nozzle performance to that of the combustor, and to establish criteria for optimizing nozzle design.

A supplemental study was conducted to assess the effect of swirl in a sudden-dump combustor configuration, and to evaluate the performance of a low-pressure-drop swirler. A swirled air inlet decreased flame length. Two modes of operation were observed. At higher fuel loadings, reaction could be initiated and maintained in the recirculation zone in the shadow of the step. The net result was a shorter overall flame length. The low-pressure drop swirler yielded a shorter flame length relative to the higher pressure drop devices.

TABLE OF CONTENTS

<u>Section</u>	<u>Title</u>	<u>Page</u>
1.0	Introduction.....	1
2.0	Experimental Facilities.....	4
	2.1 Dilute Swirl Combustor.....	4
	2.2 Two-Color Laser Anemometer.....	5
	2.3 Droplet Sizing.....	9
	2.4 Emissions.....	14
3.0	Results.....	15
	3.1 Element A: Droplet Sizing Capability.....	15
	3.2 Element B: Combustor Tests.....	31
	3.3 Element C: Supplemental Study.....	42
	References.....	48
Appendix A:	Summary of Personnel.....	51
Appendix B:	Summary of Presentations and Publications.....	52
Appendix C:	Significant Interactions.....	53



DTIC
ELECTE
S OCT 9 1986 **D**
B

Approved by	
NTIS	✓
DTIC	
By	
DIA	
A-1	
Dist	
A-1	

LIST OF FIGURES

<u>Figure</u>	<u>Caption</u>	<u>Page</u>
1	Dilute Swirl Combustor	6
2	Two-Color Laser Anemometer (LA)	7
3	Spray Chamber	11
4	Spray Diagnostics	11
5	Droplet Sizing Measurements	25
	a) Interference Test	
	b) Axial and Radial Variation of SMD	
	c) Liquid Mass Distribution	
	d) Comparison of Rosin Rammler and Model Independent Distributions	
	e) Shadow Photographs	
6	Combustor Tests	36
	a) Spray Characterization	
	b) Spray Asymmetry Results	
	c) Combustor Results	
7	Dump Combustor Results	45
	a) Combination 1	
	b) Combination 2	
	c) Combination 3	

LIST OF TABLES

<u>Table</u>	<u>Title</u>	<u>Page</u>
I	Optical Parameters for Visibility	19
II	Berglund-Liu Operating Conditions	19
III	Calibration Results, Visibility	22
IV	Combustor Test Conditions	33
V	Dump Combustor Test Combinations	44
VI	Dump Combustor Results Summary	44

SECTION 1

INTRODUCTION

Continuous flow combustion systems are both turbulent and strongly backmixed. Such flows are classified as complex because of the complicated fluid dynamics in contrast to simple flows which, while turbulent as well as laminar, do not have zones of recirculation (Launder, 1978). Examples of practical continuous flow combustion systems of direct interest to the Air Force are gas turbine and ramjet combustors.

Development of modern combustion devices is aided by numerical modeling of the combustor aerodynamics and heat release processes. In two-phase systems, the modeling of the dispersed phase is also being attempted (Crowe, 1982). One difficulty in developing a modeling capability in two-phase flows is the absence of detailed experimental measurements within flowfields of interest to verify the model and guide its improvement (Mostafa and Elghobashi, 1983).

Nonintrusive optical methods have been developed to spatially characterize the mean and turbulent motion of the gas phase of complex flow devices (Brum and Samuelsen, 1984). However, techniques to spatially resolve the dispersant phase have been applied neither routinely nor with great success. To support modeling efforts, spatially-resolved measurements of both size and the velocity of the liquid droplet are required.

The goal of the present AFOSR grant at the UCI Combustion Laboratory was to develop laboratory model combustors and experimental methodology suitable for the acquisition of the desired information. In a previous grant (78-3586), a premixed laboratory combustor, the Opposed Jet Combustor, was developed and a data base was established in both a gaseous non-reacting and reacting system as well as a hydrodynamic water system. In addition, a non-

premixed model swirl-stabilized laboratory combustor, the Dilute Swirl Combustor (DSC), was developed and tested, and a data base was established for non-reacting as well as reacting gaseous-fired conditions. The present grant was directed to operating the DSC on spray-atomized liquid fuels, to establishing a droplet sizing capability that would lead, over the five-year duration of the grant, to in situ measurements of drop size and drop velocity as well as gas velocity within the DSC, and to the study of turbulent transport in swirl-stabilized, liquid-fuel spray-atomized reacting flows. In particular, the objectives of the program were:

- (1) To develop and verify a capability to conduct in situ measurements of droplet size and velocity,
- (2) To operate the DSC with a liquid, spray-atomized twin-fluid nozzle, and
- (3) To conduct supplementary studies in support of Air Force laboratory interests in complex flows.

To meet these objectives, the program was divided in a task organization consisting of three elements:

- Element A: Droplet Sizing Capability
- Element B: Combustor Tests
- Element C: Supplemental Study

The experimental facilities developed to support the research are described in the following section. The results are presented in Section 3.0 for each of the elements delineated above. Finally, a summary is provided in Section 4.0.

The present program was terminated at the end of the first year due to a shift of support by the AFOSR to an emphasis on reacting flows of reduced complexity and relative simplicity in contrast to swirling flows. Hence, the original goal of the program (acquisition and analysis of fuel droplet distributions in swirl-stabilized combustors) was not realized. However, substantial products of the program were realized. Namely:

- Valuable comparisons of droplet sizing methods were completed.
- A comparison of nozzle performance to combustor performance was demonstrated.
- The effect of a low pressure swirler on a model laboratory dump combustor was established.

SECTION 2

EXPERIMENTAL FACILITIES

2.1 Laboratory Combustor

The Laboratory Combustor Facility (LCF) provides air flow sufficient to produce a reference velocity of 15.24 mps (50 ft/sec) in a 80 mm (3-inch) duct, and flow rates of gaseous fuels to yield overall equivalence ratios exceeding 2.0. Details of the test stand are available (Peterson and Himes, 1978).

The combustor is a model laboratory complex flow combustor developed in a series of tests (Brum et al., 1982; Brum and Samuelsen, 1982; Samuelsen, 1984) performed in conjunction with a previous AFOSR grant (78-3586). The configuration, presented in Figure 1, features an aerodynamically controlled, swirl-stabilized recirculation zone. The housing consists of an 80 mm I.D. cylindrical stainless steel tube that extends 32 cm from the plane of an air-assist nozzle. Rectangular, flat windows (215 x 306 mm) are mounted perpendicular to the horizontal plane on both sides of the combustor tube to provide a clear optical access for laser measurements. For photographic analyses and flow visualization, the stainless steel duct is replaced with an 80 mm I.D. cylindrical quartz tube.

A set of swirl vanes (57 mm O.D.) is concentrically located around a 19 mm O.D., centrally positioned, fuel delivery tube. Dilution and swirl air are metered separately. The dilution air is introduced through flow straighteners in the outer annulus. The swirl air passes through swirl vanes with one hundred percent (100%) blockage which imparts an angle of turn of 60° to the flow. For the swirl-to-dilution air flow ratio of 1.66 used in the present study, the swirl number obtained by integrating across the swirl vanes is 1.3; that obtained by integrating the total inlet mass flux is 0.5.

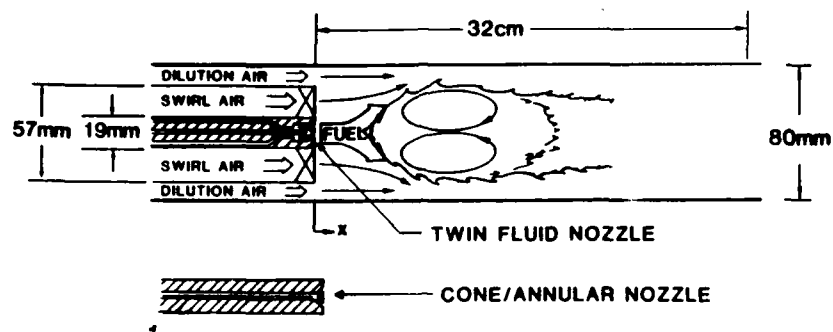
The air-assist nozzle used in this evaluation was designed by Parker Hannifin Corporation to fill a requirement for a low flow two-phase nozzle with a high degree of atomization for use in an atmospheric, laboratory combustor. The nozzle consists of two principal components. The outer body houses a set of swirl vanes and one complete air circuit. Within this, a fuel insert is fitted which contains a hollow tube surrounded by a set of swirler units on the outside surface. In conjunction with a shroud, the insert forms a second air circuit. Fuel is prefilmed on the inner surface of the shroud, separating the two air circuits, by radial injection of fuel through three small ports, located 120° apart, in the tip of the hollow fuel insert.

The combustor aerodynamic and temperature fields, obtained by two-component laser anemometry and thermocouple probe, are presented in Figure 1b for the baseline nozzle and combustor operating conditions (Wood et al., 1984). The recirculation zone extends one duct diameter downstream and consists, for this combination of swirl strength and nozzle condition, of a double vortex surrounding a positive velocity on the centerline. The thermal map shows a uniform, high temperature core with a radially diverging steep gradient to a relatively cool outer flow.

2.2 Laser Anemometer(LA)

The two-color laser anemometry (LA) system is shown in Figure 2. The beam from a 200 mW Argon-ion laser (Lexel Model 75) is collimated and passed through a prism to separate the various wavelengths. The two most intense beams, green (514 nm) and blue (488 nm) are each passed through a series of optics in which they are polarized and split into two beams of equal intensity 50 mm apart. An upstream 40 MHz frequency shift (TSI model 915 Bragg Cell) is applied to one of each pair of beams in order to avoid directional ambiguity

a) Geometry



b) Streamline and Temperature Fields ($U_{ref} = 7.5$ mps, $\phi = 0.5$, $A/F = 3.0$)

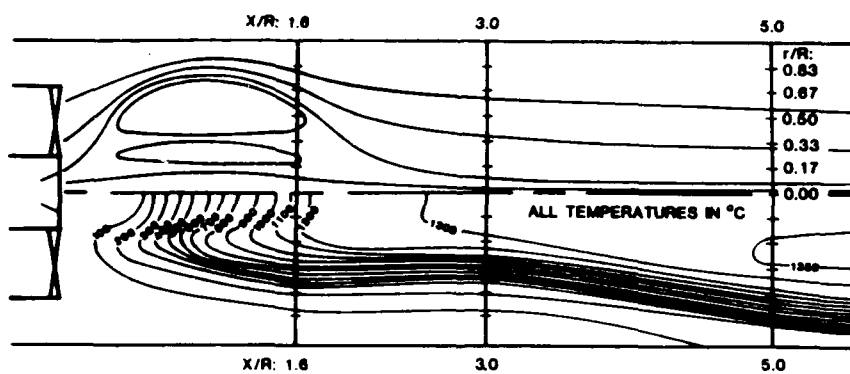


Figure 1. Dilute Swirl Combustor (Wood et al., 1984)

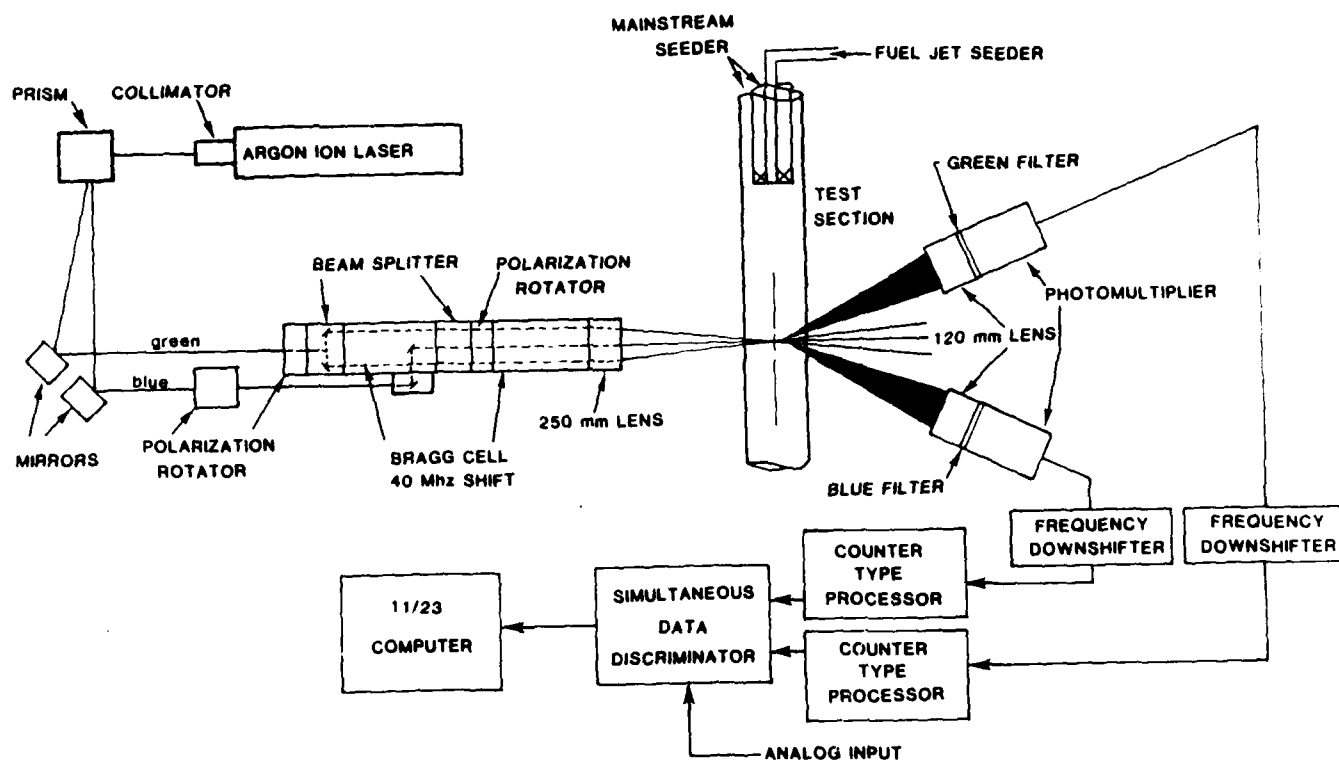


Figure 2. Two-Color Laser Anemometer (Brum 1983; Brum et al., 1983)

that would otherwise result from the highly turbulent recirculating flow. The four beams (blue pair in the vertical plane and green pair in the horizontal plane) are then focused through a 250 mm lens to a common point within the test section. This results in set of perpendicular interference fringes spaced at 2.6 μm for the green beams (vertical fringes) and 2.5 μm for the blue beams (horizontal fringes) which are responsive to the axial and tangential velocity components respectively.

Receiving optics consist of a 120 mm lens focused onto a 0.25 mm diameter photomultiplier tube aperture (via an appropriate dichromate filter to selectively pass either the blue or green light). These optics are placed at an angle of 20° off direct forward scatter which results in a probe volume of 0.022 mm³ and cross-sectional area perpendicular to the axis of measurement of 0.10 mm². However, due to the requirement imposed by the processing electronics that both axial (u) and tangential (w) velocity components be obtained simultaneously, the effective probe cross-section is much less (approximately 0.03 mm²). The transmitting and receiving optics are mounted on an optical bench capable of placing the measurement volume at points throughout the stationary combustor test section.

A special electronic interface was built to interface the output of the two counter process channels (u,w) directly to a DEC PDP 11/23 computer system. This interface identifies whether or not the u and w events occur within a certain aperture time of each other (normally $\leq 50 \mu\text{s}$). If so, they are considered simultaneous, stored, and then multiplexed into the 11/23 via a parallel interface. Once the interface verifies that the 11/23 has read the data, it simultaneously resets both processor channels. The key feature of this system is that it permits a direct and instantaneous measurement of correlations such as $\overline{u'w'}$. An aperture time of 50 μs was selected since, at

the maximum bulk velocity measured (15 m/s), an equivalent spatial resolution of less than 0.75 mm is obtained.

The 11/23 computer is equipped with an internal clock having a resolution of 100 μ s which is initiated at the beginning of each run cycle. As the u, w data are received, the time of event t is combined with the raw data (u,w,t), and the data are permanently stored in an archival fashion for future reference and analysis.

The main and fuel jet flows are seeded independently, but to the same levels of concentration, with 1 μ m alumina particles. A liquid suspension atomization seeding technique is employed, developed under the previous AFOSR Grant (78-3586) and described in Ikioka et al. (1983), which produces a controllable and uniform concentration of seed particles into each of the two streams.

Details of the system are provided in Brum (1983).

2.3 Droplet Measurements

Spray Chamber. The spray facility (Figure 3) is designed to characterize a liquid fuel atomizer under noncombusting, atmospheric conditions. The chamber consists of the 34.3 cm I.D. x 152 cm long plexiglas tube positioned vertically at the center of the optical platform. The tube rests in a fuel collection basin that is connected to an exhaust system via a fuel vapor trap. The chamber and basin assembly are mounted on a precision platform permitting one degree of freedom movement in the horizontal plane for radial traverses of the spray.

The fuel nozzle is centrally positioned within the large tube in a fixture that permits vertical movement for axial traverses. This fixture is configured identically with inner portions of the combustor. The fuel nozzle is secured in the end of a 19 mm O.D. fuel delivery tube which is plumbed to

supply fuel and air to the nozzle. This is centrally located within a 57 mm O.D. tube that is supplied with metered air and can be fitted with swirl vanes.

The exhaust system draws the air and fuel downward in the chamber. The strength of the exhaust is controlled so as to evacuate at a rate just adequate to prevent the formation of a stagnant droplet cloud in the chamber.

The optical bench platform is fixed and houses the instruments used to measure spray quality. This instrumentation (Figure 4), which includes laser diffraction, laser interferometry, and shadowgraph photography, is described below. Optical access to the spray is provided through open ports which include both circular holes and slots depending on the optical technique and traversing required.

Laser Diffraction. Laser diffraction (LD) provides a measurement of droplet size distribution along a line of sight. Hence, the measurement is an integrated or ensemble-averaged measurement, usually across the spray at a given axial location. The technique relies upon light scattered from droplets traversing the laser beam (Dobbins et al., 1963; Swithenbank et al., 1977). The Sauter Mean Diameter (SMD) is calculated using a given size distribution (e.g., Rosin-Rammler) or a model-independent algorithm. In the present case, Rosin-Rammler is used. The commercial instrument employed for the present experiment, the Malvern ST2200, was operated with a 9 mm Helium-Neon beam and both the 100 mm and 300 mm focal length receiving lens. The placement of the instrument relative to the chamber is shown in Figure 4.

Although the Malvern has a standard alignment procedure, experience has demonstrated that this can be insufficient. A set of Laser Electro-Optics reticle pairs was used to verify alignment (Hirleman, 1983). The set

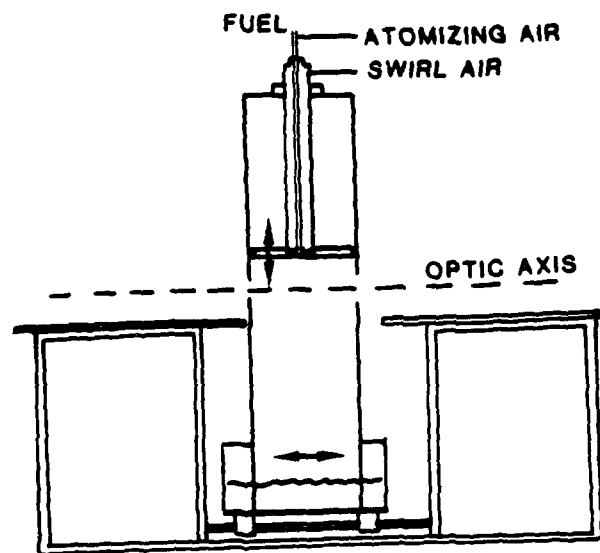


Figure 3. Spray Chamber.

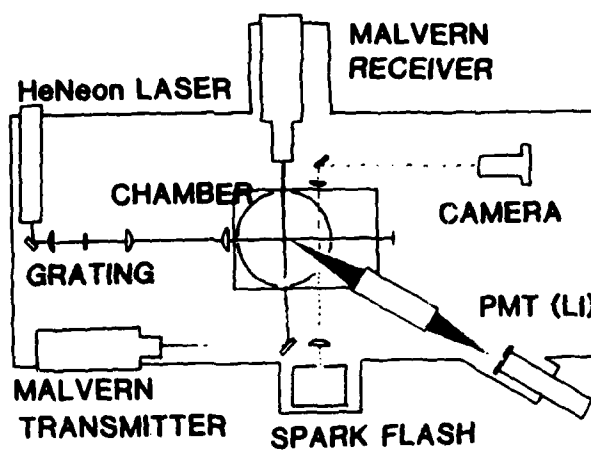


Figure 4. Spray Diagnostics

corresponds to a Rosin-Rammler size distribution of $D_{RR} = 50.0 \mu\text{m}$, $N = 2.0$ where D_{RR} is the Rosin-Rammler diameter and N is the distribution parameter. These reticles are used to (1) verify alignment, and (2) check the reproducibility of the instrument in order to verify that comparisons of data taken on a spray device over an extended period of time are valid.

Laser Interferometry. Laser interferometry (LI) provides a point measurement of droplet size, and droplet velocity (Bachalo, 1980). Interferometric sizing utilizes information contained in a Doppler burst, the scattered light signal resulting from a drop traversing a pattern of interference fringes established by the intersection of two laser beams of the same wavelength and polarity. The signal contains both velocity information (the frequency of the signal) and size information (the modulation or "visibility" of the signal intensity).

The existing LI (Figure 4) utilizes a Helium-Neon laser, a rotating grating for beam splitting and frequency shift, and a visibility processor (Spectron Development Laboratories, Model VP 1001). The visibility processor is equipped to operate either with or without visibility intensity (VI) validation, a technique which validates droplet scores that occur for the specified fringe contrast and invalidates those that occur for a fringe contrast that is degraded due, for example, to steering of the transmission beams when traversing a substantial depth into a spray (Hess, 1984).

Shadowgraph Photography. Shadowgraph photos are produced by first collecting and imaging (1:1) light from a flash source (EGG Micro-flash Model 549-11/21) onto a pinhole aperture which acts as a point source of light. Light emitted from the pinhole, is collimated by a second lens to produce a column of relatively uniform intensity light which is directed across the spray chamber. The scattered light is collected and an image pattern of the

drops is formed at a position behind the collection lens dictated by the lens focal length and the object distance. The combination used for the present tests provided a magnification factor of 2. This image is photographed by a camera (Olympus OM-2) with a bellows for enlarging the image in varying degrees of magnification in order to document the spray angle, ligament break-up at the nozzle injection plane, and detail the droplet field for a direct verification of the laser diffraction results.

Patternator. In addition to the optical instrumentation, a prototype patternator was fabricated for the present experiment to measure the spatial distribution of mass flux. The patternator consists of a linear array of 6 mm diameter vials placed at a fixed distance from the nozzle (60 mm) for a monitored duration of time. The liquid level in each vial is subsequently measured, area weighted, and converted to spatially-distributed mass flux as a measure of nozzle spray symmetry.

Monodisperse Aerosol Generator. A Berglund-Liu Vibrating Orifice Monodisperse Aerosol Generator (TSI Model 3050) is used for checking the final optical arrangement and in setting the photomultiplier tube voltage prior to spray measurement. The Berglund-Liu (BL) instrument can be made to dispense a stream of drops of a precisely known size and at a known frequency (Berglund and Liu, 1973). Two stable modes of operation are attainable. In the first mode, at relatively low frequencies (25-50 kHz, with a 20 μ m orifice and a flow rate of 0.177 cc/min) the device puts out several drops of varying sizes per cycle. The drops collide and coalesce into a single drop of a size predicted by the flow rate and frequency of stimulation within about one centimeter of the orifice. In the absence of any dispersion air, these coalesced drops are of very regular size and evenly spaced.

In the second stable mode, at higher frequencies (> 50 kHz) a single drop of a predictable size is emitted per pulse. This can be observed very close to the orifice. In this mode dispersion air can be applied to the stream and a spray of single size drops is generated. Utilizing both modes, drops from 44 to 63 μm are produced in a stream.

The BL is positioned over the optic probe volume using a precision, three directional traverse (spray chamber removed). This precise control of the Berglund-Liu position is required for setting the voltage to the PMT.

2.4 Emissions

Samples of gaseous products of combustion are extracted by a gas sample probe and conveyed, through a heated sample line, to a packaged emission analysis system (Scott Research, Model 113). Passage of the gas through an ice bath allows all concentration measurements to be taken on an equally dry basis. Nondispersive infrared analyzers (Beckman Models 315B and 325BL, respectively) are used to measure carbon dioxide (CO_2) and carbon monoxide (CO) concentrations. Total hydrocarbon (HC) concentration are measured by a flame ionization detector (Scott Research, Model 215). Oxygen (O_2) concentration is measured by a paramagnetic analyzer (Scott Research, Model 150).

SECTION 3

RESULTS

3.1 Element A: Droplet Sizing Capability

3.1.1 Introduction

The visibility sizing method was first applied to sprays utilizing light collected in the forward direction, that is, diffracted light (Farmer, 1972). Size information lost in the required beam stops limited the measurable size range considerably. Also, the shallow angle of intersection of the two laser beams, required to obtain adequate fringe spacing to measure drop diameters of interest ($> 5 \mu\text{m}$), results in a large probe volume when collection is made in the forward direction. This limits the application of this method to low density sprays.

For sprays of non-opaque liquids, Bachalo (1980) developed the necessary theory for off-axis light collection using refracted light. The optimal angle for collection is approximately 30° off the forward optic axis and out of the plane of interaction of the incident beams. The improvement made it possible to extend the measurable size range of the visibility method to 5 to 2500 μm in discrete steps with a dynamic range typically less than 10:1. Further, the size of the probe volume became more manageable as the collection optics allowed the probe volume to be significantly reduced.

The visibility technique has been successfully used to size streams of monodispersed droplets, but has encountered difficulty in sizing polydispersed sprays (Seeker et al., 1982; Ferrenberg, 1983). The principal source of the difficulty can be attributed to the nonuniform and irregular attenuation of the two beams forming the interference fringe pattern. To validate the visibility signal in polydisperse sprays, a second size determination --

intensity validation (IV) -- has been proposed (Hess, 1984).

The intensity validation (IV) technique utilizes the amplitude of the pedestal of the doppler signal to make a second measurement of size, independent of that determined by visibility. Most accurate application of this technique requires that the incident beam intensity be precisely known. Scattering intensity then becomes a direct function of scatterer's diameter (to a power) for a given collection optic arrangement. Two features of the spray environment and the measurement system make the incident light intensity an elusive quantity. First, even if the intensity of the transmitted beam into the spray could be identified, attenuation of the beam by the portion of the spray on the transmitter side of the probe volume would reduce it. Second, the Gaussian nature of the laser beams used in the measurement system provides a situation in which incident intensity is a function of the path of the droplet through the probe volume. Attenuation of the beam by the spray is corrected by automatic adjustment of the photomultiplier tube voltage by the signal processor to yield a signal amplitude consistent with a droplet having a visibility between 47 and 53%. The second problem is handled by setting limits on the intensity check such that passage of the droplet within 0.7 of the peak intensity portion of the beams will scatter adequate light to be accepted. Some error is introduced into the measurement because of these concessions. Calibration of the system in conjunction with the spray to be measured is helpful in recognizing influences of the first problem.

The research results reported here describe the application of visibility with intensity validation (IV) to a spray generated by an advanced air assist nozzle. The utility of the method is evaluated by comparing its performance to two more widely accepted but limited techniques, laser diffraction (LD) and shadowgraph photography. Diffraction measurements are made to give the mean

size and size distribution of the spray along a line of sight through the spray. Shadow photographs are taken at selected positions within the spray to provide a visual means of determining drop size. These methods yield information in different forms, but comparisons are possible.

3.1.2 Approach

The visibility sizing technique was evaluated initially using the Berglund-Liu (BL). First, single size drops were produced to aid in establishing final alignment of the receiver, to observe the effect of grating rotation on the quality of the size measurement, and to set the voltage to be applied to the PMT in the absence of beam attenuation by the spray. Second, the BL was used in conjunction with the Parker Hannifin nozzle to ascertain the effect of spray interference on the size measurement. The nozzle was first positioned on the transmitted beam side of the probe volume, then on the collector side.

The optical configuration was then tested using the Parker Hannifin nozzle as the subject. Both visibility and LD were utilized, allowing direct quantitative comparison between the techniques. Shadow photographs were also taken for visual confirmation of results.

System Calibration. The optic arrangement for the experiment was such that resolution of drops with diameters between 8 and 85 microns could be expected. (By using other tracks on the diffraction grating or other collection apertures this range can be extended.) The primary optical parameters are listed in Table I.

Three BL frequencies were used with a single flow rate and a single orifice size. Conditions are listed in Table II (the fourth frequency listed, 23 kHz, was used for the interference tests only). At these three frequencies single size drops could be observed approximately 10 mm from the BL orifice.

Using an oscilloscope, the PMT placement could be optimized to most clearly focus the doppler burst from the drops. The PMT voltage could also be precisely set for Intensity Validation (IV) using tabulated visibility and corresponding intensity values (El-Shanawahy and Lefebvre, 1980; Rizk and Lefebvre, 1983). The procedure was repeated for each of the three frequencies to ascertain whether the optimal PMT voltage changed depending upon where along the visibility curve the calibration was conducted.

At each frequency, once the voltage had been set, the BL drop size was measured using visibility alone, and then using visibility with intensity validation (IV). The visibility/IV system was then used at 4 settings of the rotating grating to observe the effect of the grating rotation on the size determination.

Interference Test. With the spray chamber removed, the BL was positioned over the probe volume using the 3 directional traverse. The Parker Hannifin nozzle was positioned on the transmitter side, half way between the transmission focusing lens and the BL. The nozzle exit was located 10 mm above the optic axis; the BL discharged at 13 mm above the probe volume. The BL was operated in the stream mode using the lowest frequency mode of drop generation. The Parker Hannifin nozzle was operated with deionized water (filtered to 25 μm) at a flow rate of 3.2 kg/hr. Two nozzle air:water (A/W) mass ratios were tested, 1.5:1 and 0.75:1. Interference tests conducted on the receiver side were identical except that the Parker Hannifin nozzle had to be raised to 30 mm above optic axis to clear the solid angle of the receiving optic. The Parker Hannifin spray and the BL both discharged into the collection basin in the absence of confinements.

Table I: Optical Parameters for Visibility

Fringe Spacing	14.2 μm
Probe Volume Diameter	200 μm
Probe Volume Length	400 μm
Collection Angle	30°
Collection F/#	4.39
PMT Aperture	200 μm
Index of Refraction (water)	1.33

Table II: Berglund-Liu Operating Conditions

Fluid	Deionized Water filtered to 0.5 μm
Volume Flow Rate	0.177 cc/min
Orifice Diameter	20 μm
Stimulation Signal Type	Square Wave
Stimulation Strength	20 Volts peak-to-peak
Frequency (Drop Diameters)	25.6 kHz (60 μm) 45.5 kHz (50 μm) 64.5 kHz (44 μm) 23.0 kHz (63 μm)

Nozzle Evaluation. The air assist nozzle was operated at one setting ($\dot{m}_w = 3.2$ kg/hr; A/W = 1.5:1) for evaluation of the spray within the spray chamber. The nozzle was checked for axial variation of Sauter Mean Diameter using the LD Malvern system. Then, at two axial positions, radial traverses of the spray were made, measuring drop size and axial velocity with the LI system. These traverses were in increments of 5 mm. The rotating grating was used only as necessary to shift the velocity data to optimal positions within the frequency band filters on the VP-1001 processor. This helped to minimize the number of data runs required at a given location in the spray to cover the full velocity range of the droplets.

As many as four separate runs were required to cover the velocities of the droplets observed at a particular location in space. This results from collection limitations imposed by the frequency band filters used on the signal processor to improve the signal-to-noise ratio and to limit rolloff error. A full radial traverse of the spray required 14 (at 30 mm axial), and 15 (at 50 mm axial) data sets. The rotating grating was useful in minimizing the overlap of data collected from two or more band filters.

Data are taken as a velocity-size pair. Up to 3072 pairs can be taken in one run. The raw data are adjusted in two ways before being combined to yield an SMD or a weight distribution. First, the effective probe volume varies as a function of the size of the drop. Due to the Gaussian nature of the laser beams larger drops traversing the edges of the probe volume may scatter enough light to exceed the processor threshold; smaller drops traversing this area may not, however. When using intensity validation, the size of the intensity band also becomes a factor. To compensate for the probe volume variation, correction schemes have been introduced (Roberds et al., 1979; SDL, 1982) to properly weight the observed counts. Such a correction is applied to each

data set. Second, the number of corrected counts must be divided by the velocity associated with each size in order to compare the data to spatial measurements (see ASTM, 1982). The velocities used are mean velocities generated for thirteen size brackets (each is 6 μ m wide) for each data set.

The Sauter Mean Diameter is calculated from the visibility/IV measurements at each spatial location by combining all contributing data sets (as many as four are required). A composite SMD is also determined at two axial positions (30 mm and 50 mm from the nozzle face). These are generated by combining all contributing data sets (14 at 30 mm, 15 at 50 mm). The SMD is calculated as

$$SMD = \frac{\sum_{i=1}^M (d_i)^3 \dot{N}_i / \bar{V}_i}{\sum_{i=1}^M (d_i)^2 \dot{N}_i / \bar{V}_i}$$

where M is the total number of contributing data sets,

d_i is the diameter of drop i,
 \dot{N}_i is the number of corrected counts of drops
 with diameter d_i per time of collection,
 \bar{V}_i is the mean velocity associated with the range
 of drop diameters (6 μ m wide) containing
 diameter d_i .

3.1.3 Results

System Calibration. System calibration consisted of aligning the receiver and setting the PMT voltage using the BL in a stable stream mode. Results on determining drop size for three frequencies of the BL using visibility and visibility with IV are presented in Table III. The PMT voltage levels determined by using the tabulated visibility and intensity ranges for each of the three drop sizes are within 0.5% of their mean value. The effect

of rotating the grating on the visibility/IV size measurement of the BL drops has also been evaluated. Results (Table III) indicate that rotation of the grating has no significant effect on the size measurement.

Table III: Calibration Results, Visibility

B-L frequency (kHz)	B-L calculated diameter (μ m)	Visibility diameter (μ m)	PMT Voltage (VDC)	Visibility/IV Diameter (μ m)				
				No Grating Rotation	1200 RPM clockwise	9000 RPM clockwise	1200 RPM counter CW	9000 RPM counter CW
25.6	60	56	385	60	56	57	57	57
45.5	50	45	382	48	47	47	48	47
64.5	44	41	382	38	44	44	47	45

Interference Measurements. Interference test results are presented in Figure 5a. Only transmission side interference is illustrated. No effect on the measurement was observed when the interference was on the receiver side. In the "OFF" condition, the Parker Hannifin nozzle is flowing air only (at the test condition). In the "ON" condition, the nozzle is flowing water and air at full operating condition. The visibility generated size distribution is broadened when the water/air spray is on for the lower air/water ratio of 0.75. The broadening is in the direction of increased size as expected with degradation of the fringe visibility due to non-uniform interference of the P-H drops with the transmitted beams upstream of the probe volume. The IV system corrects the error. For the finer spray (higher A/W, better atomization), no effect is evident although the voltage to the PMT had to be increased to compensate for attenuation of the transmitted beams. The absence of an effect on the visibility data is attributed to a near uniform attenuation to both beams in the finer spray.

Spray Measurements. Malvern data were obtained on the air assist nozzle along the spray centerline at 5 mm intervals from 10 mm off the nozzle face to 85 mm. The obscuration of the beam was approximately 20% at all positions.

The data are presented in Figure 5b. The atomization is very fine with the SMD (as determined by a Rosin Rammler curve fit) varying from 33 to 21 μm . The dip in the curve at about 25 mm off the nozzle face is consistent with other observations (Rizk and Lefebvre, 1983) and can be attributed to several factors. First, the differential in drop velocities in the near vicinity of the nozzle, resulting from the small droplets decelerating more rapidly to terminal velocity established by the surrounding air stream, causes a local biasing of the diffraction data toward smaller sizes. Second, the spreading of a typical spray involves larger drops migrating toward the outer edges of the spray while the smaller drops remain at the center. Thus, as the measurement is made further from the nozzle the biasing is also toward small sizes.

Superimposed upon the Malvern axial data are two points from the visibility/IV runs. Each point representing a composite of separate visibility/IV data sets as described in the Approach section. The comparison in Figure 5b is not good at the 30 mm station, but more reasonable (relative to Malvern) at 50 mm from the nozzle.

Figure 5b also illustrates the variation of SMD with radial position at the two axial positions of interest. The single Malvern measurement (recall it is a line of sight determination) is also included for reference at both axial stations. At 50 mm the single Malvern determination is well within the range of the visibility/IV determinations. At 30 mm the Malvern SMD is on the low extreme of the visibility/IV SMD's, consistent with the differences observed in the axial variation.

A good comparison between the two techniques should be expected provided the Malvern SMD is representative of the spray and is in fact spatially resolved; and, the visibility/IV SMD is representative of the spray and is a

properly corrected temporal measurement. A poor correspondence between the LD and visibility/IV data at 30 mm suggests one of these conditions is not met. Two of the questions will be dismissed with limited discussion. First, the Malvern data was generated using one thousand sweeps per point. It is, therefore, considered spatially resolved (i.e. the spray transients have been averaged). Second, the visibility/IV data is temporal by its nature. The corrections applied to the measurement to account for effective variation in the size of the probe volume and to make the data comparable to a spatially resolved measurement are consistent with current practice. The questions remaining concern whether the LD or visibility/IV data are representative of the spray.

The lower limit of detection by the Malvern is approximately 6 μm for this test set up (300 mm focal length collection lens and the spray centerline is 250 mm from the lens); it is near 8 μm for the visibility/IV system. The upper limit for the visibility/IV technique is approximately ten times the lower limit. For this arrangement it is about 85 μm . The Malvern should resolve to 500 μm in its configuration. The mass distributions given by the Malvern's Rosin Rammner (RR) fit of the data at both 30 mm and 50 mm (Figure 5c) suggest that 99% of the spray mass is in drops with diameters below 90 μm , indicating the size limitations of the visibility/IV technique encompasses most of the spray.

In Figure 5c the distribution of mass is compared to that measured with visibility/IV. The LD distributions are constructed using the Malvern output from the fit of the data directly. The weight percent contained in evenly spaced size intervals (each is 6 μm wide) is plotted against the median value in each interval. The visibility/IV determined weight percents are determined by taking the corrected counts, divided by the associated time of collection

a) Interference Test

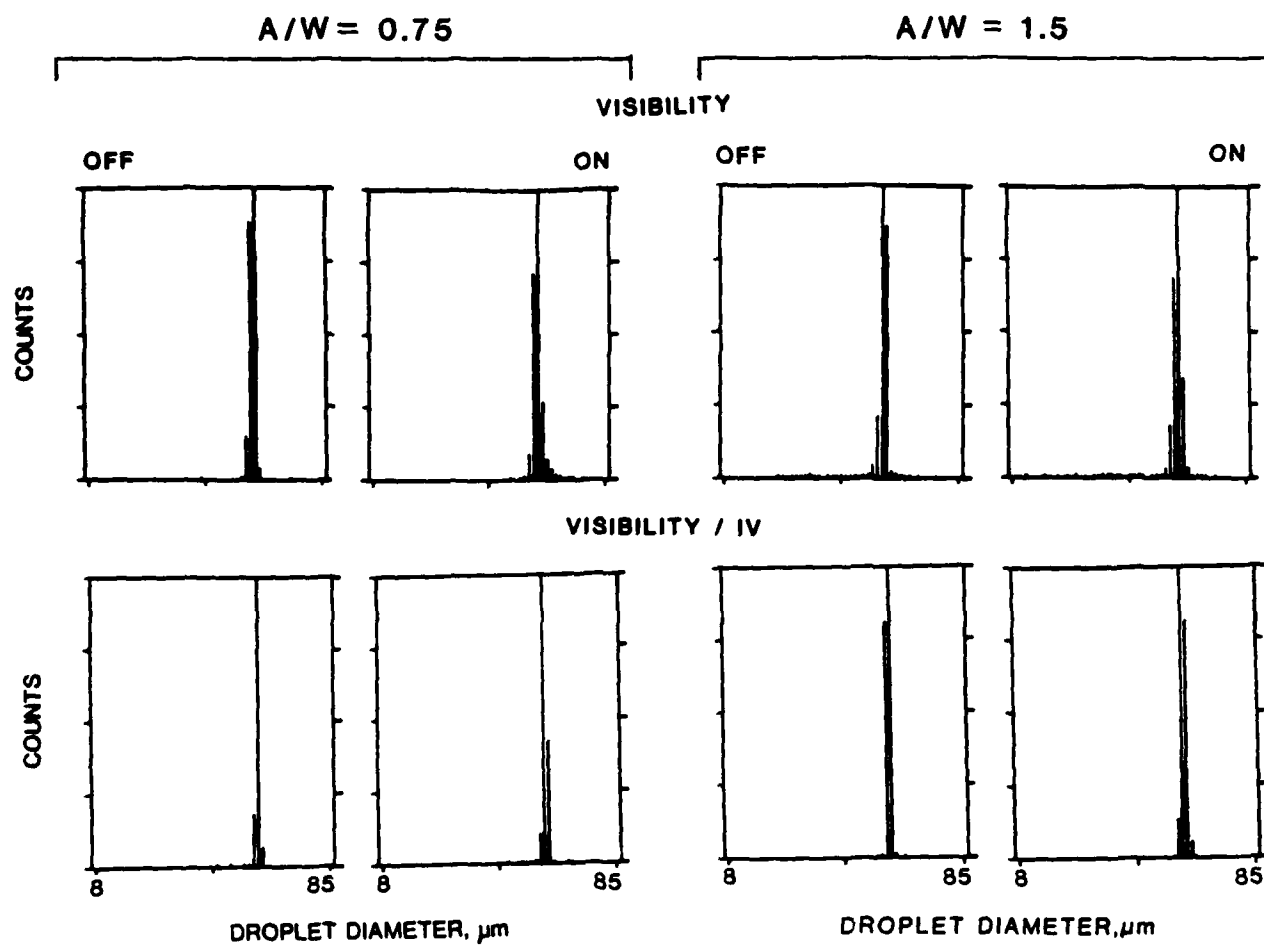


Figure 5. Droplet Sizing Measurements

b) Axial and Radial Variation of SMD

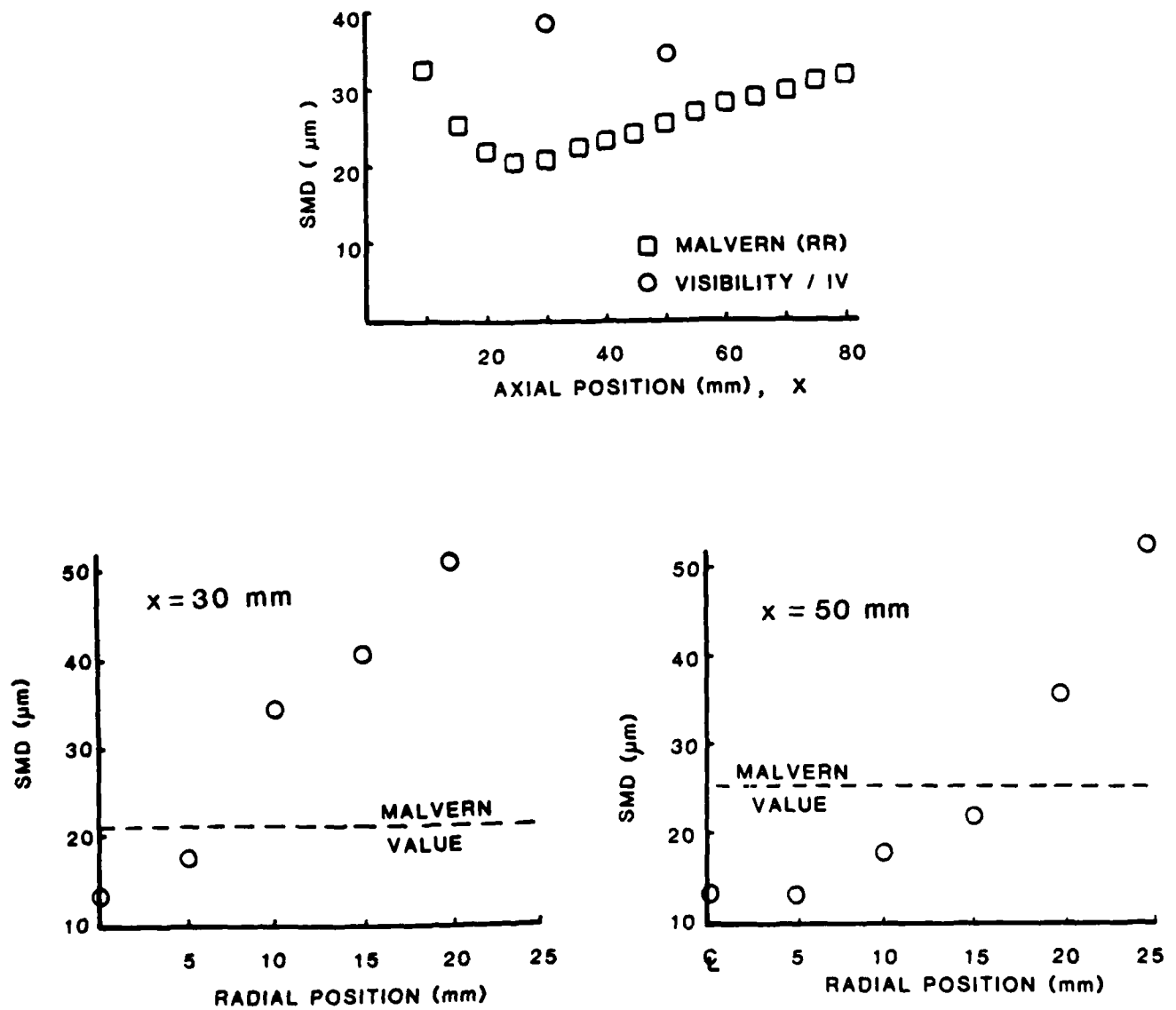
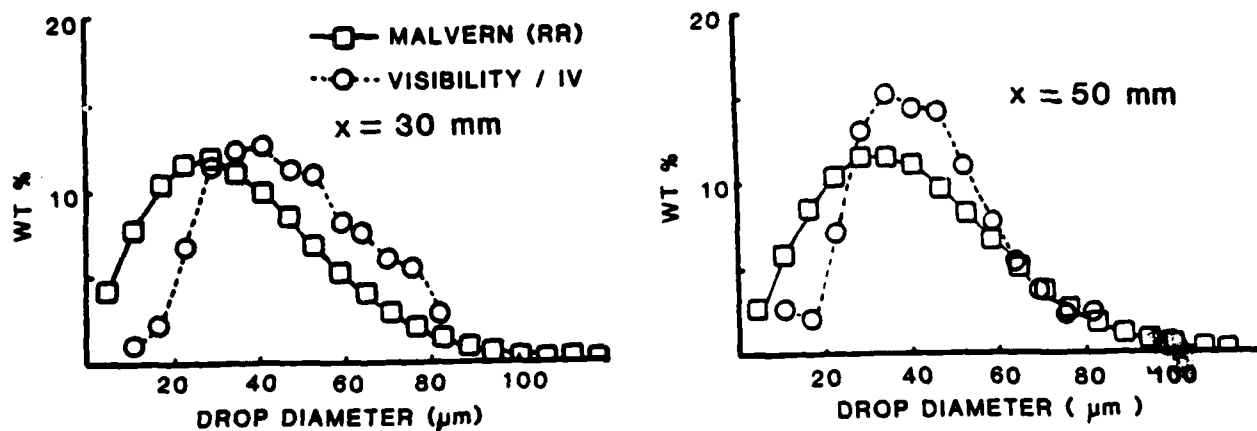


Figure 5. (continued)

c) Liquid Mass Distribution



d) Comparison of Rosin Rammler (RR) and Model Independent (MI) Distributions

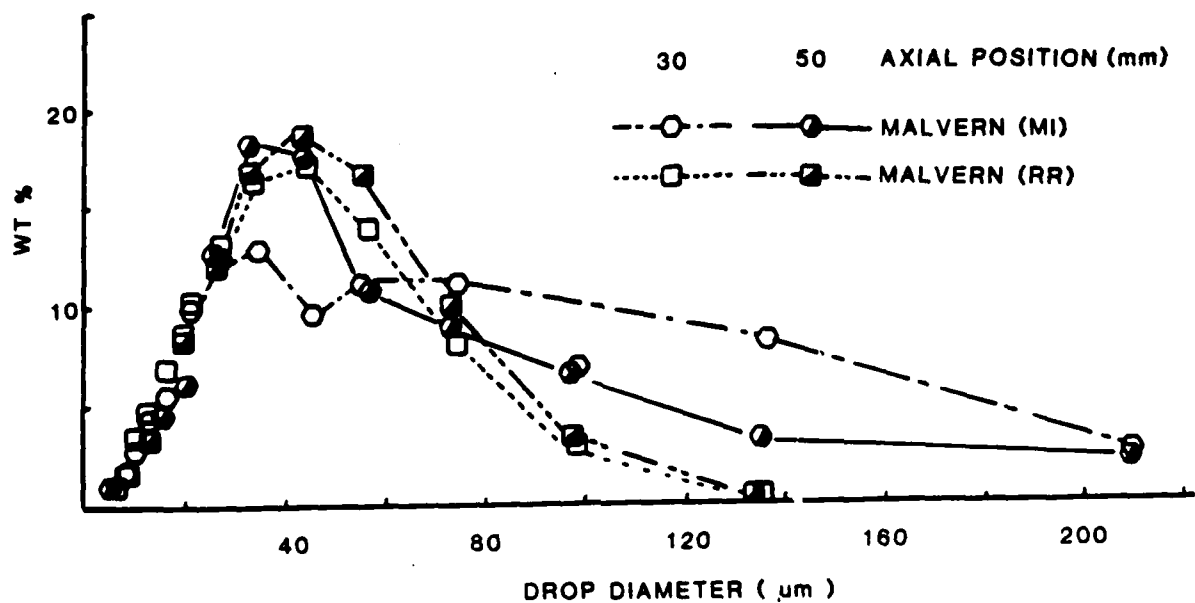


Figure 5. (continued)

and mean velocity, and summing them over the same size interval as that of the Malvern. These thirteen sums (thirteen size brackets from 8 to 85 μm) are multiplied by the cube of the median diameter of the size bracket and summed. The weight percent is the ratio of each of these thirteen sums to the total. The visibility/IV distribution at 30 mm suggests more mass is contained in larger drops than the observation by the Malvern RR. At 50 mm the two distributions differ in what each sees in the small and medium size drops.

Figure 5d examines the accuracy with which the Rosin Rammler curve fit represents the data. Plotted are the weight distributions of the same data points shown in Figure 5c. In Figure 5d, however, both the Rosin Rammler (2 parameter) algorithm and the Model Independent (15 parameter) algorithm are applied to the same data set. The size intervals used are those output for the Model Independent (MI) algorithm. They are variable, ranging from 1.4 to 101.2 μm wide. At 30 mm, the 2 point fit smoothes over an appreciable amount of the mass contained in larger drops ($\sim 17\%$). This occurs despite the fact that the fitting error was well within acceptable limits (Log Error ≈ 4.5) for the Rosin Rammler model. At 50 mm, the correspondence between the two models is excellent.

The visibility/IV and LD data at the 50 mm axial station show very good agreement, both in the spray SMD and in the weight distribution. The variations which are present suggest the visibility/IV data is closer to the Malvern Model Independent analysis than to Malvern RR. The poorer match at 30 mm is also expected in light of the Model Independent treatment of the Malvern data. The composite SMD of the visibility/IV is appreciably higher than that of the Malvern RR; but the visibility/IV SMD is in the direction suggested by the Model Independent distribution. To be effective in

providing adequate characterization of the spray at 30 mm, the visibility/IV size limitation would have had to be broadened. This would have necessitated splicing data to overlap size windows as well as velocity windows. This complication was avoided in this effort.

Typical shadowgraph photos are presented, in Figure 5e. In illustration (a) the nozzle exit conditions are captured. Liquid ligaments are clearly visible. In this region the visibility/IV technique with off axis collection is not applicable as the drops are not spherical (the LD technique will also experience error if the asphericity is not random). Illustrations (b) and (c) are shots from within the spray at 30 and 50 mm off the nozzle face, respectively. Along the nozzle centerline the resolution is very poor although some small drops are in focus. Moving away from the centerline the drop images are much more clear. Their spherical shape is apparent. The images also clearly show the presence of drops larger than 90 μm . This is consistent with the LD data when examined with the model independent algorithm.

3.1.4 Summary

The investigation demonstrates the application of a non-intrusive technique for obtaining droplet size and velocity information within a practical liquid spray device. Such measurements are useful to hardware designers as well as to those who model two-phase flow fields. Specific results of this paper are as follows:

1. A calibration device such as a single size droplet generator is indispensable in establishing the capabilities of a given interferometric sizing system. The BL was required to ascertain the PMT voltage, the influences of the rotating grating, and the effect of the spray on the measurement capability of the system. Final receiver alignment is also enhanced.
2. Use of an alternate sizing method to complement and validate the visibility measurement is necessary in a dense spray environment. The IV technique worked satisfactorily in the present case.

3. The rotating grating can be effectively used as a beam splitter for an interferometric sizing system. Further, given the restriction of having to process signals within fairly narrow frequency bands, the variable frequency shift capability associated with the rotating grating is most appealing. No deterioration of the system's sizing capability was observed.
4. The Malvern SMD was within the extremes of the radial variation of SMD generated by the visibility/IV technique.
5. The distribution of the liquid mass within the spray as measured by the LI technique was qualitatively similar to a Rosin Rammler curve fit of the Malvern data at both axial stations. AT 30 mm, however, the visibility/IV measurements suggested a higher percentage of the weight existed in larger drops, consistent with the Model Independent treatment of the Malvern data.
6. The optical configuration was selected to best cover the anticipated range of sizes from the air assist nozzle. Coverage of a broader size distribution would require moving to a different track (different line spacing) on the diffraction grating, changing the collection aperture, or other more extensive changes as well as overlapping data sets from adjacent size ranges. This "dynamic range" limitation of the visibility/IV method influenced the comparison to LD data at one axial station.
7. Shadow photographs provide a means of visually checking the sizes of drops within the spray and also indicate where visibility/IV measurements as well as LD measurements are not possible due to the asphericity of the droplets.

Results from this study are scheduled for presentation and publication in Jackson and Samuelsen (1985).

3.2 Element 8: Combustor Tests

3.2.1 Introduction

Acceptable operation of a gas turbine combustor requires the satisfaction of many criteria. For example, a combustor must (1) operate stably over a broad load envelope, (2) relight after blow out, and (3) perform within acceptable goals for particulates and gaseous emissions. Criteria such as these have been met by extensive hardware development and hardware testing. When operational problems are encountered, a design change is evoked based on deductive reasoning. Hardware tests are initiated to verify the success of

the corrective action. This approach has, over the years, created a substantial experiential data base. A major conclusion derived from this data base is the pivotal role of fuel spray quality and fuel placement in establishing the overall performance of gas turbine combustors (Lefebvre, 1983).

The need to extract more fuel from a barrel of oil and use alternative sources of fuel (shale, coal) has introduced an additional criterion to the list above, namely that combustors should be flexible with respect to fuel properties without compromising performance. Unfortunately, a departure from the present fuel property specifications portends a (1) degradation in fuel atomization, and (2) an increased time for droplet evaporation (Lefebvre et al., 1978). Hence, if fuels of relaxed specifications are to be successfully accommodated, a "fine tuning" between atomization, fuel distribution, and fuel/air contacting will be required. Such tuning will benefit from nonintrusive, in-situ measurements of the flow aerodynamics, droplet size, and droplet trajectories in combustors representative of practical devices and, ideally, in the practical configurations themselves. Fortunately, laser diagnostics are evolving that may make these measurements a reality (Chigier, 1983).

The research results represent an example of the use of spray measurements to relate nozzle performance to the performance of a swirl-stabilized combustor representative of a practical gas turbine combustor. An air-assist nozzle is first characterized using laser diffraction, shadowgraph photography, and liquid collection in a spray chamber. Second, the performance (flame shape, combustor stability, combustion efficiency, and combustor symmetry) of a model laboratory swirl-stabilized combustor is assessed as a function of nozzle operating condition.

3.2.2 Approach

The approach to the present study was to first characterize the nozzle in the spray chamber and then test the performance of the nozzle in the combustor as a function of nozzle operating condition. The test conditions are presented in Table IV. The parameters in the experiments were nozzle atomizing air-to-fuel ratio (A/F), fuel flow rate and, as a test of nozzle asymmetry, nozzle fuel insert. Two fuel inserts (A and B) were employed in the present program. Both were identical with one exception. One of the three holes in Insert A was sized smaller than the nominal hole size. As a result, Insert A had an intrinsic asymmetry. A blend of isooctane and tetralin (1,2,3,4-tetrahydronaphthalene) served as the fuel except for the asymmetry tests in the spray chamber where water was used due to the substantial quantity of liquid required. The fuel blend constituents and

Table IV: Test Conditions

Spray Characterization

Fuel: 92% Isooctane/8% Tetralin
Fuel Mass Rate: 2.2, 3.2, 4.3, 5.4, 6.1 kg/hr
Nozzle Air-to-Fuel (A/F) Ratio: 0.54, 0.75,
1.5, 2.0, 3.0, 3.5
Water Mass Flow (Asymmetry Tests): 5.4 kg/hr
Fuel Inserts: A and B

Combustor Performance

Reference Velocity: 7.5 mps
Fuel: 92% Isooctane/8% Tetralin
Fuel Mass Rate: 5.4 kg/hr
Overall Equivalence Ratio: 0.5
Nozzle Air-to-Fuel (A/F) Ratio: 0.75,
1.5, 3.0^a, 3.5

Fuel Inserts: A and B

a. Baseline Condition for Figure 6b.

mixture percentage (92% isooctane/8% tetralin) were adopted based on a parallel, soot-formation study in which pure hydrocarbons are blended to yield the smoke point (23 mm) of a shale JP-8 fuel stock (Wood et al., 1985).

Spray Characterization Tests. The spray characterization tests included the use of shadowgraph photography, laser diffraction, and liquid collection. The photography served three purposes. First, photography was used to document the droplet break-up and chamber inlet conditions at the nozzle exit including size of liquid ligaments and angles at which the filaments are injected. Second, with a lower magnification, photography provided a measure of the spray angle. Third, at high magnification, the photography provided a verification of the laser diffraction measurements.

Laser diffraction (LD) was employed for two purposes. First, conventional characterization of the nozzle was accomplished by (1) measuring the centerline variation in SMD as a function of nozzle A/F ratio, and (2) measuring the variation in SMD at a select axial plane (40 mm) as a function of nozzle fuel flow. Second, LD was used to assess whether the diffraction results would reveal an asymmetry in the spray when Insert A, with a known fuel distribution bias, was housed in the nozzle. Tests for an asymmetry in SMD were conducted by making full-diameter radial traverses at 60° increments of nozzle orientation in a 360° rotation.

Patternator tests were conducted at a single axial position. The nozzle was rotated through 360° with collections of the liquid spray made at 60° intervals. The measurements were used to assess whether the asymmetry would be revealed in measurements of mass flux.

Combustor Performance Tests. The combustor tests were conducted at 7.5 mps and an overall equivalence ratio of 0.5 (5.4 kg/hr of fuel). Still photography was used to record the flame shape and to record the spray field

at the point of injection. Full-diameter radial profiles of the gaseous products of combustion were acquired at an axial location far downstream of the nozzle face (2.5 duct diameters, $x/R = 5.0$) but sufficiently upstream (1.0 duct diameter) of the duct exit to avoid flow variations introduced by the exit plane. The full-diameter traverses were used to (1) determine the efficiency of combustion and (2) quantify the symmetry of the combustor. The symmetry test was accomplished by rotating the nozzle (the fuel tube holder can be rotated while the combustor is in operation) to two positions from the nominal: $+90^\circ$ (CW) and $+180^\circ$ (CW).

3.2.3 Results

Spray Characterization. The results of the spray characterization are presented in Figure 6a. Shadowgraph photography of the ligament break-up at the nozzle face shows clearly the improvement in atomization quality as the nozzle atomizing air-to-fuel (A/F) ratio is increased. Axial laser diffraction measurements of SMD show an increase in SMD with distance from the nozzle face. This is attributed to evaporation (El-Shanawahy and Lefebvre, 1980). The more pronounced increase at the lower A/F ratio is associated with the larger mean diameter and broadened size distribution in the spray at A/F = 0.75. This is graphically displayed in Figure 6a where the Rosin-Rammler size distributions are shown to narrow at higher A/F ratios as well as move to smaller droplet diameters. This variation with A/F ratio is even more pronounced at higher fuel flow rates. Atomization quality, as measured by the SMD, is also affected by A/F ratio and fuel flow rate, improving as these parameters are increased. (The small droplet sizes observed at high A/F ratios approach the resolution limit of the Malvern. High magnification shadowgraph photography was used to verify that the measured size distributions and Sauter Mean Diameters were correct.)

a) Spray Characterization

SHADOWGRAPH PHOTOGRAPHS OF LIGAMENT BREAKUP

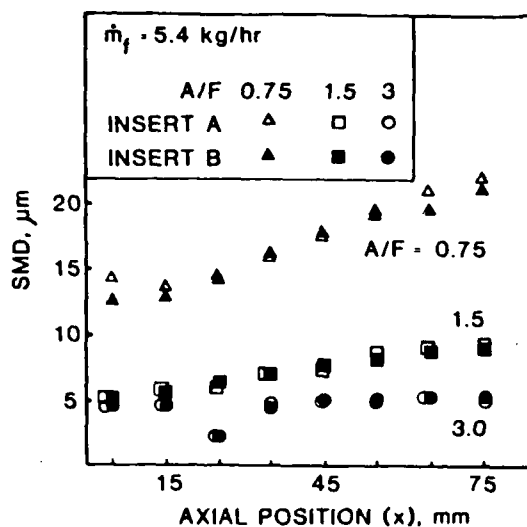


A/F = 0.54

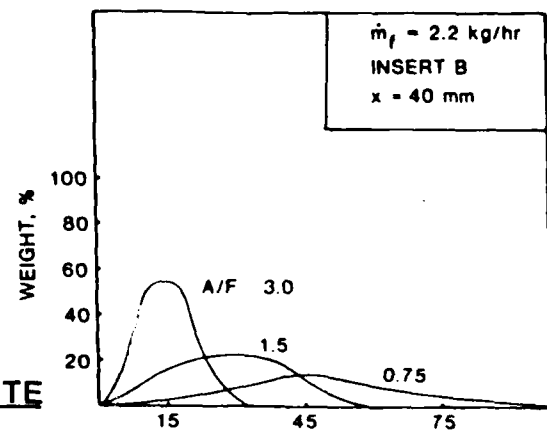


A/F = 3.00

AXIAL VARIATION IN SMD



SIZE DISTRIBUTIONS



DEPENDENCY OF SMD ON FUEL FLOW RATE

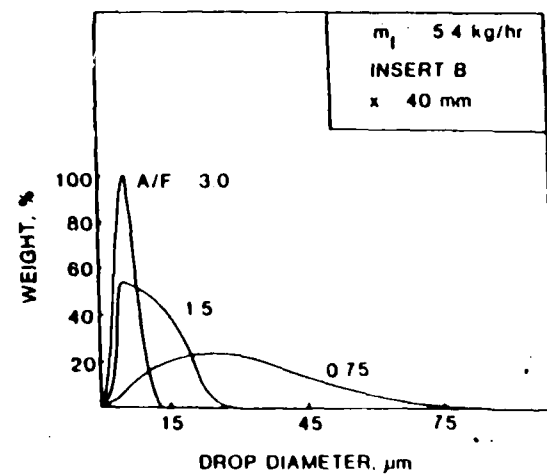
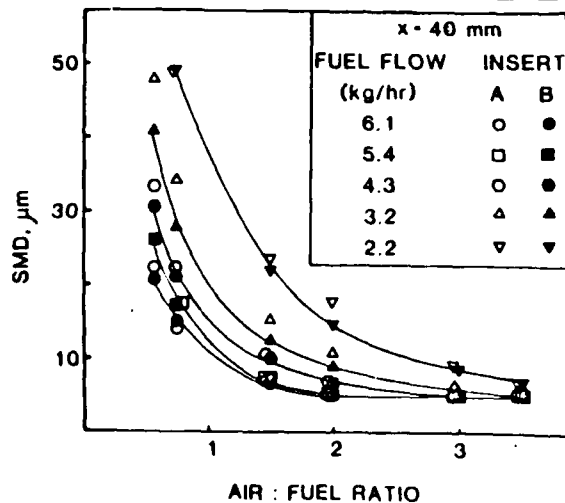
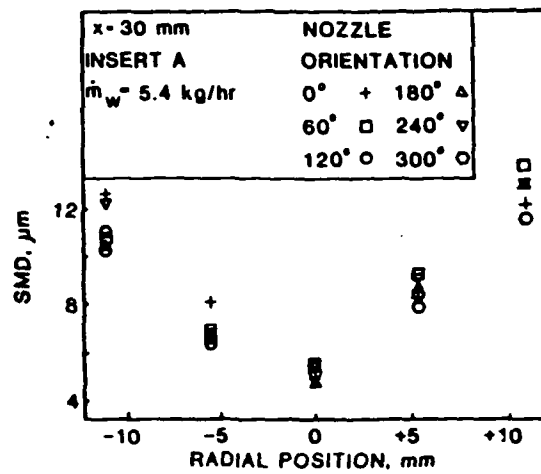


Figure 6. Combustor Tests

b) Spray Asymmetry Results

● MALVERN



● PATTENATOR

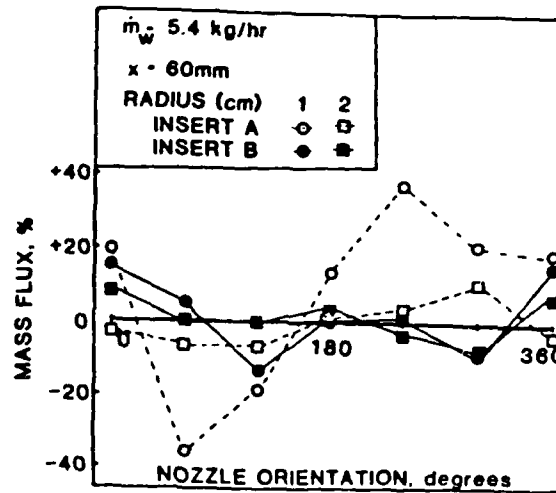
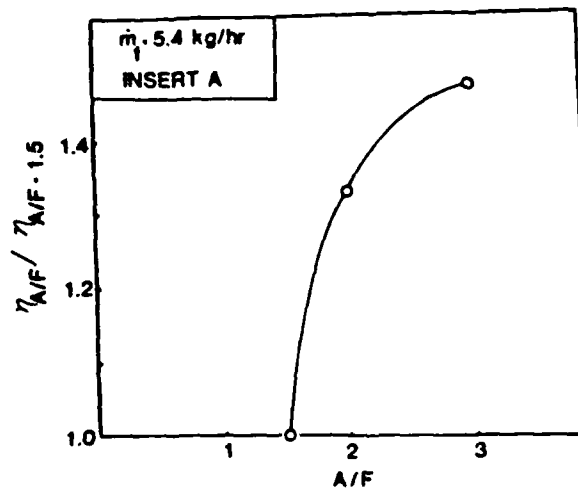


Figure 6. (continued)

c) Combustor Results

• EFFICIENCY



• SYMMETRY TESTS

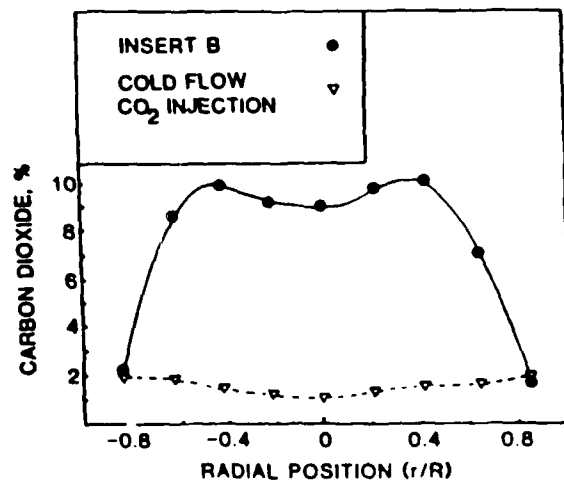
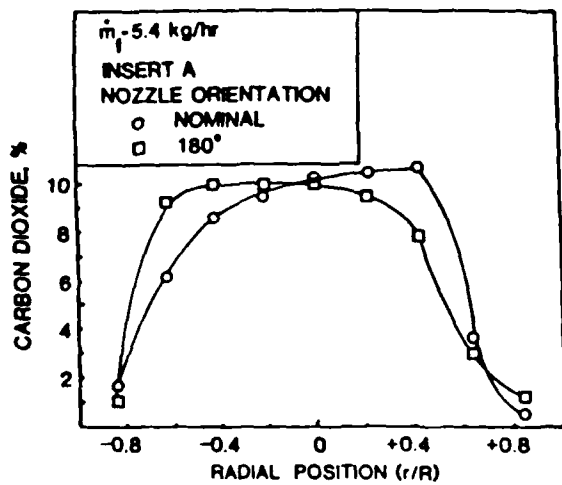


Figure 6. (concluded)

The trends described above are similar to those observed with air-blast atomizers (Rizk and Lefebvre, 1983), except an initial reduction in SMD immediately downstream of the nozzle is observed here only for the $A/F = 3.0$ case. The observation in other studies is explained by the differential in droplet velocities in the near vicinity of the nozzle as the small droplets decelerate more rapidly to the terminal velocity established by the surrounding air stream. The absence of an initial reduction in SMD for the $A/F = 1.5$ and 2.0 conditions is not fully explained through the coarse spatial resolution of the 9 mm diffraction beam is a contributing factor.

The radial variation in SMD was assessed by surveying the spray radially in both directions from the centerline at a selected axial location (30 mm). The results, presented in Figure 6b for Insert A, show that the SMD increases radially away from the centerline which is consistent with the size segregation as the smaller droplets in the radially directed spray establish an axial trajectory more rapidly than larger droplets which, due to a higher ballistic fortitude, transition less rapidly to the axial direction.

The radial variation data in Figure 6b also demonstrate whether the known fuel bias in Insert A is reflected in a SMD asymmetry in the spray. Data are presented for six nozzles orientations. The variation in SMD, although significant and systematic, does not reflect an asymmetry in droplet size and results, instead, from the uncertainty of positioning the large diffraction beam (9 mm) in the relatively small spray cone.

The patternator tests results, by contrast, establish that the fuel distribution bias of Insert A is transformed into a spray asymmetry in mass flux. Plotted in Figure 6b is the circumferential variation in mass flux at two radial stations displaced from the spray centerline by 1 and 2 cm respectively. The data plotted are normalized to the mean mass flux of the

first radial station. The variation in mass flux at the first radial station approaches -40% of the mean at 60° and +40% at 240°, 180° displaced from 60°. At the second radial station, evidence of the asymmetry is not pronounced. The variation in mass flux for Insert B, while not establishing exact symmetry, is acceptable within expected performance of practical nozzles and experimental error. These results point to the desirability of applying convolution techniques (Yule et al., 1981; Tishkoff et al., 1981) to laser diffraction measurements and/or applying laser interferometry (Mularz, 1983) to spatially resolve the droplet size and droplet velocity in order to clarify the spray asymmetry.

Combustor Performance. The combustor was first operated to assess the effect of atomizing air-to-fuel ratio (A/F) on overall flame structure. At an A/F = 0.75, the maximum nozzle atomizing air flow rate prescribed by Parker Hannifin, the flame was diffusion-type in character with a large, radiant, yellow core reaction zone. As the nozzle A/F ratio was increased, the flame transitioned to a highly intense and distributed reaction with a clearly discernable recirculation zone. At nozzle A/F ratios exceeding 3.0, the flame blew out. The combustion efficiency is presented in Figure 6c as a function of nozzle A/F ratio. The best suited nozzle A/F ratio is 3.0 for (1) this particular nozzle, (2) the aerodynamics of this particular combustor, and (3) the combustor operating conditions considered in the present experiment. These data form the foundation upon which nozzle design options can be explored to improve and optimize the nozzle performance in the present combustor.

The asymmetry of Insert A was clearly discernable in the radial profiles of emission. Representative data for carbon dioxide are presented in Figure 6c for nozzle orientations corresponding to both nominal and rotated

180°. (Note that these orientations cannot be directly compared to those in Figure 6b. In the latter, combustor flow aerodynamics were absent. In the former, combustor flow aerodynamics transport and transform the asymmetry from the nozzle to the plane of emission measurements.) The profile at 180°, a near mirror-image of that at 0°, is not symmetrically distributed around the centerline. The CO₂ emission profile for Insert B reflects the symmetry desired in a combustor of this type. To test the symmetry of the combustor in the absence of liquid fuel injection and reaction, CO₂ was injected through a simple, symmetric cone-annular nozzle (Figure 1) of the type described elsewhere (Brum and Samuelsen, 1982). The results, shown in Figure 6c, established the symmetry of the combustor under cold flow conditions.

3.2.4 Summary

The present study is an example of the use of spray measurements to relate nozzle performance to the performance of a swirl-stabilized model laboratory combustor. Such measurements will be required in the future to tailor nozzle performance to combustor aerodynamics in order to achieve a criterion of fuel flexibility in gas turbine engines. The results of the paper lead to the following conclusions:

1. Air-assist nozzles exhibit a trend of improved atomization performance with increasing nozzle air-to-fuel ratio (A/F) similar to that observed for air-blast atomizers.
2. The size distribution of the air-assist nozzle narrows with increasing increasing A/F and increasing fuel flow rate.
3. The performance of a swirl-stabilized model laboratory combustor increases with A/F due to improved atomization (lower droplet sizes and narrower size distributions) and higher fuel momentum. An A/F ratio is reached, above which the combustor cannot be stabilized and "flames-out".
4. An intrinsic asymmetry, introduced into the nozzle, was not reflected in laser diffraction measurements of SMD but rather in patternator measurements of mass flux. The nozzle asymmetry was also observed in the radial profiles of gaseous species emitted from the combustor.

5. Matching of nozzle performance to a combustor aerodynamic field will benefit from local, spatially resolved measurements of droplet size and droplet velocity both in the spray chamber and in the combustor.
6. Quantification of the combustor velocity field as a function of nozzle operating condition will be required, along with droplet size and droplet velocity measurements, to relate nozzle performance to that of the combustor, and to establish criteria for optimizing nozzle design.
7. The results provide a foundation upon which to initiate a program of optimization to establish the nozzle design best suited for the present combustor.

Results from this study were presented in Jackson and Samuelsen (1984).

3.3 Element C: Supplement Study

3.3.1 Supplemental Study

A supplemental study was conducted under the present grant to evaluate the effect of swirl on flame length in a dump combustor configuration. The work was conducted under a task for the Ramjet Division at the Wright Aeronautical Laboratories (AFWAL/PORT). An important element of the task was to test the performance of a low pressure drop swirler designed by UCI Combustion Laboratory staff. The tests were conducted using visualization as the principal means of measuring performance.

3.3.2 Approach

Studies on swirling flows in the sudden expansion dump combustor were conducted using three different swirl-vane types (70% blockage, 100% blockage, low-pressure drop helical), in two dump combustors of slightly differing area ratios yielding a total of five combustor combinations. The use of two combustors was necessary to accommodate the different swirlers which varied slightly in outer diameter and total length. The 70 and 100% blockage swirlers were evaluated in the UCI Combustion Laboratory Dilute Swirl Combustor ("DSC") with the dilution annular jet blocked. In this configuration, the DSC is a dump combustor with the step-height to radius

(h/r) and diameter ratios listed in Table V. A dump combustor ("Dump") module, used in previous tests (Samuelsen, 1984), was employed for the helical vanes. The five combustor combinations are summarized in Table V.

3.3.3 Results

Table VI summarizes the test results. The study resulted in a series of still photographs of the combustor flame for each combination. Also recorded were lean blowoff limit, flame length, as well as a written observation of the flame appearance and performance. The duct diameter and length were nominally 80 mm (3-inches) and 14 cm (36-inches), respectively.

A nominal overall equivalence ratio of $\phi = 0.70$ was selected based on the experimental results with nonswirl (Samuelsen, 1984). For nonswirl, $\phi = 0.7$ was the leanest condition the dump could be operated with acceptable stability. Higher fuel loadings were avoided to limit the heat load to the combustor test stand and laser receiving optics.

Combination 1. Combination 1 ran with a very stable flame at $\phi = 0.70$. The flame had an intense dark blue color with bright blue "swirl lines". The flame length varied between 40 and 50 cm. Careful observation of the flame revealed the outline of the centerline recirculation zone (Figure 7a). Increasing the equivalence ratio resulted in the flame shortening to 30 cm to 40 cm at $\phi = 0.71$. Just prior to this point, the combustor produced a loud rumbling sound. The shorter flame seemed to be due to the fact that the outer-torodial recirculation zone became a luminous ("reaction") zone as evidenced by the appearance of bright blue, luminous zones in the step region. In addition, the flame became attached to the dump plane. Increasing the equivalence ratio further resulted in an even shorter blue flame, but a long yellow tail formed on the combustor centerline. Lean blowoff occurred at $\phi = 0.64$.

Table V: Dump Combustor Combinations

$$\phi = 0.70$$

Combination	h/r^*	Diameter Ratio	Combustor Module	Swirl Vane Type	Dilution Air	Velocity (m/s)	Fuel Type
1	0.30	0.70	DSC	70% blockage	blocked	7.5	Propane
2	0.30	0.70	DSC	100% blockage	blocked	7.5	Propane
3	0.30	0.70	DSC	No Swirl	blocked	7.5	Propane
4	0.50	0.66	Dump	Helical	NA	7.5	Propane
5	0.50	0.66	Dump	No Swirl	NA	7.5	Propane

* h : step height ($\frac{O.D_s - I.D_s}{2}$); r : main duct radius ($\frac{O.D_s}{2}$)

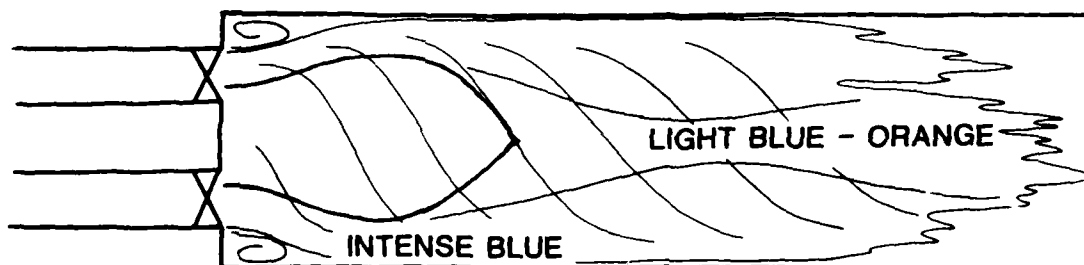
Table VI: Dump Combustor Results Summary

$$\phi = 0.70$$

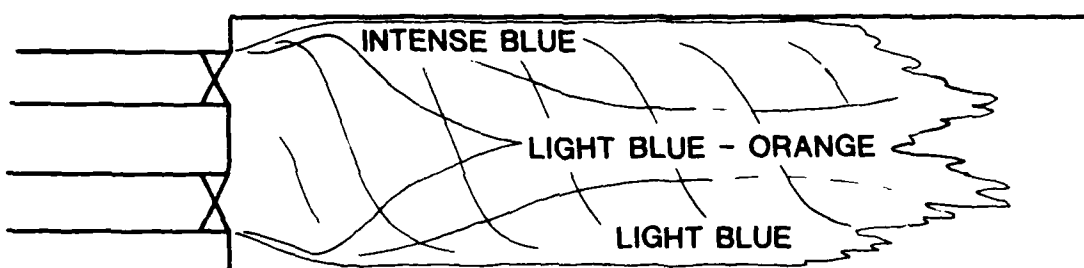
Combination	h/r^*	Diameter ratio	Lean Blowoff Limit ϕ	Rich Blowoff ϕ	Flamlength $\phi = 0.70$ (cm)	Short Operation	
						ϕ	Flamlength (cm)
1	0.30	0.70	0.64	-	40 - 50	0.71	30 - 40
2	0.30	0.70	0.61	-	35 - 40	0.84	25 - 30
3	0.30	0.70	0.59	-	50 - 60	-	-
4	0.50	0.66	0.40	-	25 - 30	-	-
5	0.50	0.66	0.48	-	60	-	-

* h : step height ($\frac{O.D_s - I.D_s}{2}$); r : main duct radius ($\frac{O.D_s}{2}$)

a) Combination 1



b) Combination 2



c) Combination 3

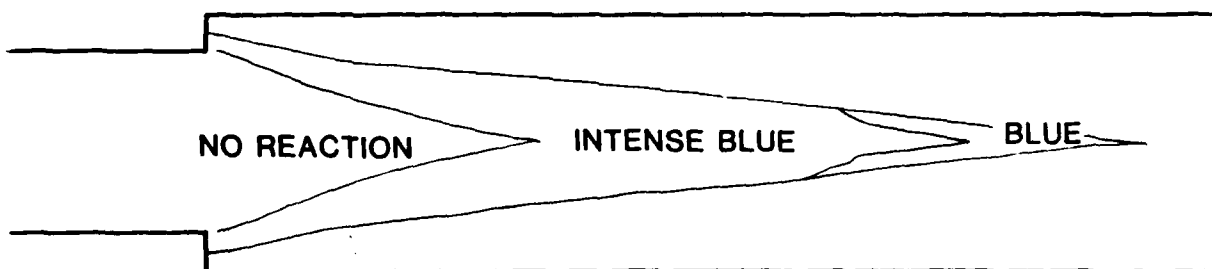


Figure 7. Dump Combustor Results

Combination 2. Combination 2 was very similar in appearance to combination 1. The flame, however, appeared much hotter and more intense. The flame length was shorter, varying between 35 cm and 40 cm. The shape of the centerline recirculation zone (Figure 7b) exhibited a discontinuity in transition from a fattened upstream curvature to a pointed downstream cone (Figure 7b), whereas the shape of the recirculating zone produced by the 70% blockage vanes was a more continuous, football shape. This combination also exhibited a "short flame-length" operation mode which occurred at $\phi = 0.84$. Lean blowoff occurred at $\phi = 0.61$.

Combination 3. Combination 3 with no swirl was much different in shape than either of the swirl combinations. The flame was long (50-60 cm) and conical (Figure 7c). Lean blowoff occurred at $\phi = 0.59$, a value lower than that achieved by either the 70 or 100% blockage.

Combination 4. Combination 4 with the helical, low-pressure drop swirl vanes created a flamelength of 25 cm to 30 cm. This was shorter than that of either combination 1 or 2 at $\phi = 0.70$. This was due to the fact that this combustor, at $\phi = 0.70$, ran in the short flame mode with the outer recirculation zones reacting. Due to the dump combustor module design, it was not possible to identify the equivalence ratio at which the flame detached from the dump plane for this combination. The flame appearance was similar to combinations 1 and 2. Lean blowoff occurred at $\phi = 0.40$, the lowest blowoff limit of any combination.

Combination 5. Combination 5 with no swirl was identical to combination 3. The flamelength was 60 cm. Lean blowoff occurred at a lower value ($\phi = 0.48$) due to the higher step height.

3.3.4 Summary

Swirled inlet air in the sudden expansion dump combustor has shown to decrease flamelengths and increase flame intensity. Lean blowoff limits were lower for the nonswirl cases, and lowest in the module with a greater step height to radius ratio (0.50 vs 0.30). The short operation mode, visually observed in combinations 1, 2, and 4, may pose material heating problems. The helical, low-pressure drop vane yielded the shortest flame length.

Further studies should address the combustion efficiency for each of the different combinations.

REFERENCES

- ASTM STD E 799-81 (1982). "Data Criteria and Processing for Liquid Drop Size Analysis."
- Bachalo, W.D. (1980). "Method for Measuring the Size and Velocity of Spheres by Dual-Beam Light-Scatter Interferometry," **Applied Optics**, 19, 363-370.
- Berglund, R.N. and Liu, B.Y.H. (1973). "Generation of Monodisperse Aerosol Standards", **Environmental Science and Technology**, 7, 147-153.
- Brum, R.D. (1983). "Evaluation of a Candidate Model Complex Flow Combustor Using Instantaneous Two-Color Laser Anemometry", Ph.D. dissertation, University of California, Irvine, UCI Combustion Laboratory Report ARTR-83-5, Mechanical Engineering, University of California, Irvine, Ca, 92717.
- Brum, R.D., Ikioka, L.M., and Samuelsen, G.S. (1982). "Assessment of Candidate Combustor Configurations as Test Beds for Modeling Complex Flow," presented at the AIAA/ASME Fluids, Plasma, ASME Paper 82-HT-36, St. Louis, MO.
- Brum, R.D., and Samuelsen, G.S. (1982). "Assessment of a Dilute Swirl Combustor as a Bench Scale, Complex Flow Test Bed for Modeling, Diagnostics, and Fuels Effects Studies," presented at the AIAA/SAE/ASME Joint Propulsion Conference, AIAA Paper 82-1263, Cleveland, OH.
- Brum, R.D., Seiler, E.T., LaRue, J.C., and Samuelsen, G.S. (1983). Instantaneous Two-Component Laser Anemometry and Temperature Measurements in a Complex Flow Model Combustor, AIAA Paper 83-0334, presented at the AIAA 21st Aerospace Sciences Meeting, Reno, NV.
- Brum, R.D., and Samuelsen, G.S. (1984). "Two-Component Laser Anemometry Measurements of Non-Reacting and Reacting Complex Flows in a Swirl-Stabilized Model Combustor," presented at the 1984 Winter Annual ASME Meeting, Symposium on Experiments in Reactive and Non-Reactive Flows, New Orleans, December. To be published in **Experiments in Fluids**.
- Chigier, N. (1983). "Drop Size and Velocity Instrumentation," **Prog. Energy Combust. Sci.** 9, 155-177.
- Crowe, C.T. (1982). "Review - Numerical Models for Dilute Gas-Particle Flows", **J. of Fluids Engineering**, 104, 297-303.
- Dobbins, R.A., Corcco, L., and Glassman, I. (1963). "Measurement of Mean Particle Sizes of Sprays from Diffractively Scattered Light," **AIAA Journal**, 1, 1882-1886.
- El-Shanawahy, M.S., and Lefebvre, A.H. (1980). "Air-blast Atomization: Effect of Linear Scale on Mean Drop Size," **J. Energy**, 4, 184-189.
- Farmer, W.M. (1972). "Measurement of Particle Size, Number Density, and Velocity using a Laser Interferometer", **Applied Optics**, 11.

Ferrenberg, A.J. (1983). "Liquid Rocked Injector Atomization Research," ASTM Symposium on Liquid Particle Size Measurement Techniques.

Hess, C.E. (1984). "A Technique Combining the Visibility of a Doppler Signal with the Peak Intensity of the Pedestal to Measure the Size and Velocity of Droplets in a Spray," presented at the AIAA 22nd Aerospace Sciences Meeting, AIAA Paper 84-0203, Reno, NV.

Hirleman, E.D. (1983). "On-Line Calibration Technique for Laser Diffraction Droplet Sizing Instruments," presented at the 28th International Gas Turbine Conference, ASME Paper 83-GT-232.

Ikioka, L.M., Brum, R.D., and Samuelsen, G.S. (1983). "Laser Anemometer Seeding Technique for Combustion Flows with Multiple Stream Injection, **Combustion and Flame**, 49, 155.

Jackson, T.A., and Samuelsen, G.S. (1984). "An Evaluation of Fuel Spray Performance in a Swirl Stabilized Combustor Using Optical Methods for Drop Sizing", AIAA/SAE/ASME, 20th Joint Propulsion Conference, AIAA Paper 84-1318.

Jackson, T.A., and Samuelsen, G.S. (1985). "Spatially Resolved Droplet Size Measurements", to be presented at the 1985 ASME International Gas Turbine Conference, Houston, March; accepted for publication in **Journal for Engineering of Gas Turbines and Power**.

Launder, B.E. (1978). "Measurements and Prediction of Complex Turbulent Flows," University of California, Davis.

Lefebvre, A.H., Mellor, A.M., and Peters, J.E. (1978). "Ignition/Stabilization/Atomization: Alternative Fuels in Gas Turbine Combustors," in Bowman, C.T., and Birkeland, J. (Eds.), Alternative Hydrocarbon Fuels: Combustion and Chemical Kinetics, Progress in Astronautics and Aeronautics, 62, 137-159.

Lefebvre, A.H. (1983). Gas Turbine Combustion, Hemisphere Publishing Corporation, 13 and 371.

Mostafa, A.A., and Elghobashi, S.E. (1983). "Prediction of a Turbulent Round Gaseous Jet Laden with Vaporizing Droplets," Western States Section/CI.

Mularz, E.J. (1983). "Detailed Fuel Spray Analysis Techniques," AGARD Conference Proceedings No. 353, Combustion Problems in Turbine Engines, AGARD-CP-353, 15-1 to 15-10.

Peterson, P.R., and Himes, R.M. (1978). Opposed Jet Combustor Experimental Facility, UCI Combustion Laboratory Report ARTR-78-8, Mechanical Engineering, University of California, Irvine, CA, 92717.

Rizk, N.K., and Lefebvre, A.H. (1983). "Influence of Atomizer Design Features on Mean Drop Size," **AIAA Journal**, 21, 1139-1142.

Roberds, D.W., Brassier, C.W., and Bomar, B.W. (1979). "Use of a Particle Sizing Interferometer to Study Water Droplet Size Distribution," **Optical Engineering**, 18, May-June.

Samuelson, G.S. (1984). "Mechanisms of Exhausts Pollutants and Plume Formation in Continuous Combustion," Final Report, AFOSR Grant 78-3586, UCI Combustion Laboratory Report ARTR-84-7, Mechanical Engineering, University of California, Irvine, CA, 92717.

Spectron Development Laboratories, Inc., (1982). "Integrated Particle Sizing System Operator's Manual: Data Management System", Vo. IV, SDL No. 82-51029, Sept.

Seeker, W.R., Clark, W.D., and Samuelson, G.S. (1982). "The Influence of Scale and Fuel Properties on Fuel-Oil Atomizer Performance." Proceedings of the 1982 Joint Symposium on Stationary Combustion NO_x Control, Volume 2, Electric Power Research Institute Report, EPRI CS-3182, V2, July.

Swithenbank, J., Beer, J.M., Taylor, D.S., Abbot, D., and McCreath, G.C. (1977). "A Laser Diagnostic Technique for the Measurement of Droplet and Particle Size Distribution," in Zinn, B.T. (Ed.), Experimental Diagnostics in Gas Phase Systems, Progress in Astronautics and Aeronautics, 53, pp. 421-447.

Tishkoff, J.M., Hammond, D.C., and Chraplyvy, A.R. (1981). "Diagnostic Measurement of Fuel Spray Dispersion," presented at the ASME Winter Annual Meeting, ASME Paper 80-WA/HT-35.

Wood, C.P., Smith, R.A., and Samuelson, G.S. (1984). "Spatially-Resolved Measurements of Soot Size and Population in a Swirl-Stabilized Combustor," to be published, Twentieth Symposium (International) on Combustion, The Combustion Institute, University of Michigan, Ann Arbor.

Yuel, A.J., Ah Seng, C., Felton, P.G., Ungut, A., and Chigier, N.A. (1981). "A Laser Tomographic Investigation of Liquid Fuel Sprays," Eighteenth Symposium (International) on Combustion, The Combustion Institute, pp. 1501-1509.

Appendix A
Summary of Personnel

Faculty

Dr. G.S. Samuelson
Dr. J.C. LaRue

Staff Research Associate

Mr. C.P. Wood

Graduate Students

Mr. T.A. Jackson
Mr. V.P. Roman
Mr. K.C. Hopkins
Ms. E.T. Seiler

Undergraduate Students

Ms. R.E. Charles
Mr. T.E. Bond
Mr. R.R. Ijams
Mr. M.J. Plapp

Appendix B

Summary of Presentations and Publications

Presentations

Jackson, T.A., and Samuelsen, G.S. (1984). An Evaluation of Fuel Spray Performance in a Swirl Stabilized Combustor Using Optical Methods for Drop Sizing. Presented at the AIAA/ASME/SAE 20th Joint Propulsion Conference, AIAA paper 84-1318, Cincinnati, June.

Samuelsen, G.S., LaRue, J.C., and Seiler, E.T. (1984). Instantaneous Two-Component Laser Anemometry and Temperature Measurements in a Complex Reacting Flow. Presented at the Second International Symposium on Applications of Laser Anemometry to Fluid Mechanics, Lisbon, July.

LaRue, J.C., Samuelsen, G.S., and Seiler, E.T. (1984). Momentum and Heat Flux in a Swirl-Stabilized Combustion. Presented at the Twentieth Symposium (International) on Combustion, University of Michigan, August.

Brum, R.D., and Samuelsen, G.S. (1984). Two-Component Laser Anemometry Measurements of Non-Reacting and Reacting Complex Flows in a Swirl-Stabilized Model Combustor. Presented at the 1984 Winter Annual ASME Meeting, Symposium on Experiments in Reactive and Non-Reactive Flows, New Orleans, December.

Jackson, T.A., and Samuelsen, G.S. (1985). Spatially Resolved Droplet Size Measurements. Accepted for presentation at the 30th ASME International Gas Turbine Conference, ASME Paper 85-GT-38, Houston, March.

Publications

Brum, R.D., and Samuelsen, G.S. (1984). Two-Component Laser anemometry Measurements of Non-Reacting and Reacting Complex Flows in a Swirl-Stabilized Model Combustor. In So, R.M.C., Whitelaw, J.H., and Lapp, M. (Eds.), Experimental Measurements and Techniques in Turbulent Reactive and Non-Reactive Flows, ASME Applied Mechanics Division AMD-Vol. 66.

LaRue, J.C., Samuelsen, G.S., and Seiler, E.T. (1985). Momentum and Heat Flux in a Swirl-Stabilized Combustor. Twentieth Symposium (International) on Combustion, The Combustion Institute, in press.

Samuelsen, G.S., LaRue, J.C., and Seiler, E.T. (1985). Instantaneous Two-Component Laser Anemometry and Temperature Measurements in a Complex Reacting Flow. Proceedings of the Second International Symposium on Applications of Laser Anemometry to Fluid Mechanics, in press.

Jackson, T.A., and Samuelsen, G.S. (1985). Spatially Resolved Droplet Size Measurements. Journal of Engineering for Gas Turbines and Power, in press.

Brum, R.D., and Samuelsen, G.S. (1986). Two-Component Laser Anemometry Measurements of Non-Reacting and Reacting Complex Flows in a Swirl-Stabilized Model Combustor, Experiments in Fluids, in press.

Appendix C

Significant Interactions

U.S. Air Force

Wright Aeronautical Laboratories, WPAFB

- Dr. Mel Roquemore
 - Turbulent Transport
 - Spray Diagnostics
 - Swirl
- Dr. Don Stull
 - Dump Combustor
 - Swirl Generator

Engineering Services Center, Tyndall AFB

- Major Tom Lubvozinski
- Captain Paul Kersh
 - Dilute Swirl Combustor

AFOSR Investigators

- Dr. Norman Chigier
- Dr. Arthur Lefebvre
 - Spray Diagnostics
- Dr. Jim Peters
 - Fuels
 - Spray Mechanics

Industry

- Parker Hannifin, Mr. Harold Simmons
 - Spray Characterization
- UTRC, Mr. Jan Kennedy, Dr. Alan Eckbreth
 - Spray Characterization
- General Electric, Mr. Jack Taylor
 - Spray Characterization
- Allison Dr. Hukam Mongia
 - Spray Characterization

Agencies

- NASA Lewis, Dr. Ed Mularz; Dr. Jim Holdeman
 - Spray Characterization

DATE
FILMED
= 8